# Ocean Raman scattering in satellite backscatter UV measurements

Alexander P. Vasilkov,[1] Joanna Joiner,[2] James Gleason,[2] and Pawan K. Bhartia[2]

Received 20 February 2002; accepted 20 May 2002; published 11 September 2002.

[1] Vibrational Raman scattering by liquid water (ocean Raman scattering) significantly contributes to the filling-in of solar Fraunhofer lines observed by satellite backscatter ultraviolet (buv) instruments in the cloudless atmosphere over clear ocean waters. A radiative transfer model accounting for this effect in buv measurements has been developed and the results compared with observations from the European Space Agency's Global Ozone Monitoring Experiment (GOME). The model extends existing models for ocean Raman scattering to the UV spectral range. Ocean Raman scattering radiance is propagated through the atmosphere using a concept of the Lambert equivalent reflectivity and an accurate radiative transfer model for Rayleigh scattering. The good agreement between model and observations suggests that buv instruments may be useful for estimating chlorophyll and dissolved organic matter contents. *INDEX TERMS:* 4552 Oceanography: Physical: Ocean optics; 3360 Meteorology and Atmospheric Dynamics: Remote sensing; 0360 Atmospheric Composition and Structure: Transmission and scattering of radiation; *KEYWORDS:* ultraviolet radiation, Ring effect, Raman scattering. **Citation:** Vasilkov, A. P., J. Joiner, J. Gleason, and P. K. Bhartia, Ocean Raman scattering in satellite backscatter UV measurements, *Geophys. Res. Lett.*, *29*(17), 1837, doi:10.1029/2002GL014955, 2002.

## 1. Introduction

[2] The filling-in and depletion of solar Fraunhofer lines, known as the Ring effect [*Grainger and Ring*, 1962], is a significant component of radiances observed by backscatter ultraviolet (buv) satellite instruments. Rotational-Raman scattering (RRS) of atmospheric $N_2$ and $O_2$ is a major contributor to the Ring effect. Models for RRS have been developed and have compared well with observations from the satellite backscatter ultraviolet (SBUV) spectrometer and the GOME [see e.g., *Joiner et al.*, 1995; *Chance and Spurr*, 1997; *Vountas et al.*, 1998].

[3] Properties of RRS can be exploited to retrieve cloud pressure from buv observations [*Joiner and Bhartia*, 1995; *de Beek et al.*, 2001]. Accurate modeling of the Ring effect is crucial for retrieval of cloud pressure as well as trace gas (e.g. $NO_2$ and $SO_2$) amounts from instruments such as GOME and the Ozone Monitoring Instrument (OMI) to fly on NASA's EOS Aura satellite [see e.g., *Vountas et al.*, 1998]. Cloud pressures derived from these instruments may be used to improve retrieval of total column ozone and other trace gases.

[1]Science Systems and Applications Inc., Lanham, Maryland, USA.
[2]Laboratory for Atmospheres, Goddard Space Flight Center, Greenbelt, Maryland, USA.


0094-8276/02/2002GL014955$05.00

[4] Vibrational Raman scattering in the ocean has been not been included in these studies. Ocean Raman scattering has been observed and modeled in the visible spectral range [e.g., *Marshall and Smith*, 1990; *Haltrin and Kattawar*, 1993; *Sathyendranath and Platt*, 1998; *Gordon*, 1999] and causes filling in of solar Fraunhofer lines.

[5] To quantify the effect of Raman scattering, *Joiner et al.* [1995] defined a filling-in factor to be the fractional difference between the observed radiance and that computed using elastic scattering only. Figure 1 shows the ratio of the observed filling-in from SBUV continuous spectral scan measurements (taken approximately once per month from 1979–1986) to that computed using the *Joiner et al.* [1995] atmospheric RRS model over cloud free scenes. The filling-in over clear waters can exceed 40% of that expected from the atmosphere. There is spatial anti-correlation between the excess filling-in and chlorophyll concentrations derived from e.g. SeaWiFS (http://seawifs.gsfc.nasa.gov/SEAWIFS.html). This suggests that the excess filling-in is a result of ocean Raman scattering.

[6] In this paper we extend existing models for ocean Raman scattering to the UV spectral range and describe a method to account for the effect in satellite buv measurements. The model, intended for use with OMI, is compared with existing data from the GOME.

## 2. Ocean Raman Model

[7] Top-of-atmosphere (TOA) radiance measured by a satellite instrument, $I$, can be partitioned into two components: one consisting of photons that never penetrate into water, $I_a$, and photons scattered at least once in water $I_w$, i.e., $I = I_a + I_w$, where the subscripts $a$ and $w$ will be used to denote atmosphere and ocean, respectively. We generalize the definition of the filling-in factor [*Joiner et al.*, 1995] to include the contribution of ocean Raman scattering:

$$k(\lambda) = \frac{I - I'}{I'} = \frac{I_a - I'_a}{I'_a + I'_w} + \frac{I_w - I'_w}{I'_a + I'_w} \equiv k_a(\lambda) + k_w(\lambda), \quad (1)$$

where primed quantities denote radiances calculated with only elastic scattering, $k_a(\lambda)$ is the filling-in factor calculated without Raman scattering in water, $k_w(\lambda)$ is the filling-in excess due to Raman scattering in water. All radiances are convolved with an appropriate instrument band pass, thus the filling-in factor is an instrument-dependent quantity. Here, we compute $k_a(\lambda)$ using the RRS model of *Joiner et al.* [1995]. This scheme uses the concept of Lambertian equivalent reflectivity (LER) that assumes a Lambertian reflecting surface imitating aerosol scattering, Fresnel reflection from the ocean surface, and backscatter in water.

[8] The ocean Raman scattering filling-in factor, $k_w(\lambda)$, can be expressed as a sum of two terms. The first term, $k_{w1}(\lambda)$, is positive and represents energy transferred form

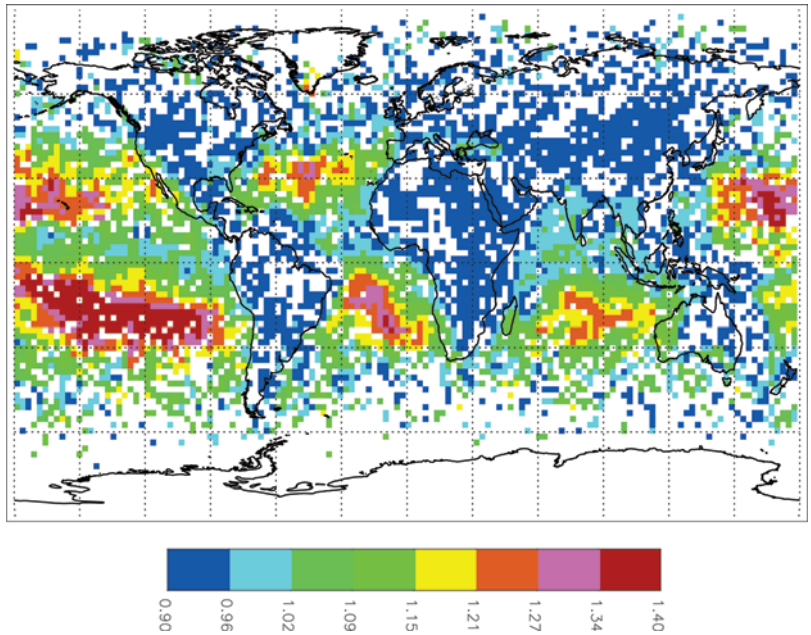


**Figure 1.** Excess filling-in at the Ca K line for scenes with reflectivity <25%.

shorter excitation wavelengths, $\lambda_e$, to an observed wavelength $\lambda$:

$$k_{w1}(\lambda) = \frac{\int F_0(\lambda_e)\rho_w^R(\lambda,\lambda_e)d\lambda_e}{\overline{F}_0(\lambda)\rho_a(\lambda)} \approx \frac{\rho_w^R(\lambda,\lambda_e)\int F_0(\lambda)d\lambda_e}{\overline{F}_0(\lambda)\rho_a(\lambda)}, \quad (2)$$

where $F_0$ is the solar flux, $\overline{F}_0$ is the solar flux convolved with the instrument bandpass, and $\rho$ is the TOA reflectance. The integration in (2) is performed over excitation wavelengths of the ocean Raman scattering band [*Haltrin and Kattawar*, 1993]. The second term, $k_{w2}(\lambda)$, is negative and is due to Raman scattering that transfers energy from the observed wavelength to longer wavelengths: $k_{w2}(\lambda) = \rho_w^R(\lambda', \lambda)/\rho_a(\lambda).\rho_a(\lambda)$ is calculated using the LER concept.

[9] Assuming clear skies, the Raman TOA reflectance can be expressed in the form:

$$\rho_w^R(\lambda,\lambda_e) = \frac{T(\lambda_e,\theta_0)T(\lambda,\theta)R_{rs}(\lambda,\lambda_e)}{1 - S_b(\lambda_e)A} \quad (3)$$

where $T$ is the atmospheric transmittance, $\theta_0$ is the solar zenith angle (SZA), $\theta$ is the viewing zenith angle, $R_{rs}$ is the remote-sensing reflectance just above the ocean surface (Fresnel reflection not included), $S_b$ is the fraction of solar flux backscattered by the atmosphere toward the ocean surface, and $A$ is the LER. The remote sensing reflectance can be expressed through the irradiance reflectance, $R$, just beneath the ocean surface. We assume isotropic angular distribution of the upwelling Raman-scattered radiance.

[10] To calculate the Raman reflectance just beneath the ocean surface, we use the major term of the Raman reflectance formula derived by *Sathyendranath and Platt* [1998]. After some transformation this formula becomes

$$R(\lambda,\lambda_e) = \frac{b_b^R(\lambda_e)}{a(\lambda_e) + b_b(\lambda_e) + \left[\mu_d(\lambda_e)/\mu_u^R(\lambda) + b_b(\lambda)\right]}, \quad (4)$$

where $b_b^R$ is the Raman-backscattering coefficient, $a$ is the absorption coefficient, $b_b$ is the backscattering coefficient, $\mu_d \approx 0.75$ and $\mu_u^R \approx 0.5$ are the mean cosines for downwelling irradiance and upwelling Raman-scattered irradiance. To calculate the Raman reflectance of the ocean we need to specify the inherent optical properties (IOP) of seawater: $b_b^R$, $a$, and $b_b$.

[11] The Raman-backscattering coefficient and its spectral dependence are obtained from *Marshall and Smith* [1990]. The total IOP are the sums of the IOP of pure seawater and scattering and absorbing water constituents.

[12] At present, there is no consensus on the pure water absorption coefficient in the UV. Pure water absorbance substantially determines the magnitude of Raman reflectance. A comparison of the available measurements of pure water absorption in the UV is shown in Figure 2. Here, we

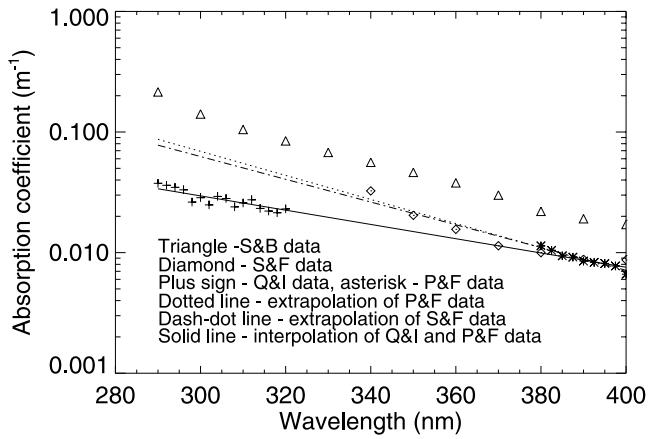


**Figure 2.** Available pure water absorption measurements-Q&I: *Quickenden and Irvin* [1980]; P&F: *Pope and Fry* [1997]; S&F: *Sogandares and Fry* [1997]; S&B: *Smith and Baker* [1981].

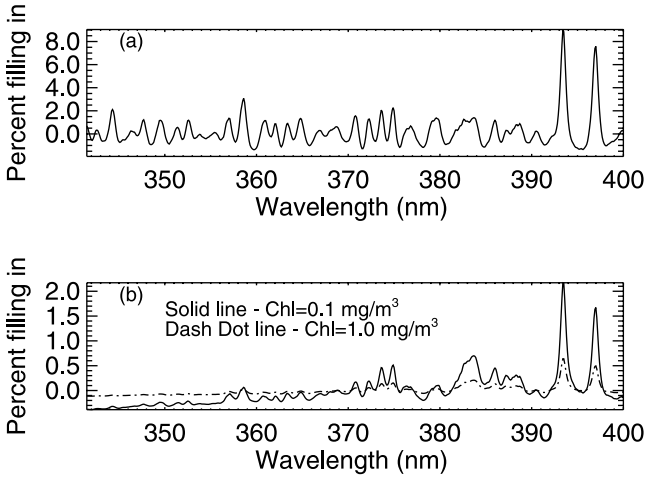


**Figure 3.** (a) Atmospheric Raman filling-in; (b) oceanic Raman filling-in.

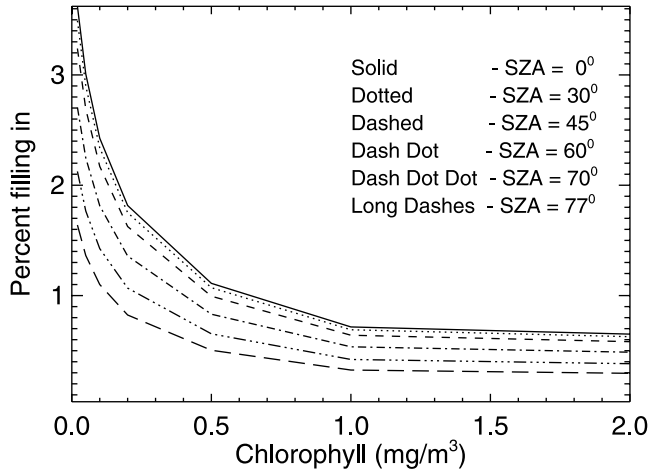


**Figure 4.** Chlorophyll dependence of $k_w$ for different SZA.

use a logarithmic interpolation between measurements of *Quickenden and Irvin* [1980] and *Pope and Fry* [1997] unless specified otherwise. The pure seawater backscattering coefficient is taken from *Smith and Baker* [1981].

[13] A model of IOPs in the UV is similar to one proposed by *Vasilkov et al.* [2001]. The model was updated by specifying the chlorophyll-specific absorption coefficient as a function of chlorophyll concentration. The particulate matter absorption is expressed through chlorophyll concentration, $C$, and the chlorophyll-specific absorption coefficient: $a_p(\lambda) = Ca_p^*(C, \lambda)$. Parameterization of the chlorophyll-specific absorption coefficient in the UV is similar to the one developed in the visible by *Bricaud et al.* [1995]: $a_p^*(C, \lambda) = A(\lambda)C^{-B(\lambda)}$. The coefficients $A(\lambda)$ and $B(\lambda)$ were determined from CalCOFI data sets (*G. Mitchell and M. Kahru*, private communication, 2001).

[14] The IOP model contains three input quantities: the dissolved organic matter (DOM) absorption coefficient at a reference wavelength, $a_0$, the particulate matter backscattering coefficient at a reference wavelength, $b_0$, and chlorophyll concentration, $C$. In order to formulate the model in terms of a single parameter, we use the Case 1 water model [*Morel*, 1988]. According to the model, the DOM absorption at 440 nm is 20% of the total absorption of pure seawater and particulate matter pigments. The backscattering coefficient is expressed through the total scattering coefficient $b_0 = 0.015b(550)$. A value of the particulate total scattering coefficient at 550 nm was approximated as $b(550) = 0.3C^{0.62}$ [*Morel*, 1988]. Thus, all the input parameters are expressed as a function of a single input quantity - chlorophyll concentration.

## 3. Ocean Raman Model Calculations

[15] In this section we present some results of calculations of the filling-in factor, $k_w$. All the calculations were performed within the wavelength range of 340–400 nm using a triangular band pass with a full-width-half-maximum of 0.45 nm which is the approximate resolution of OMI. Spectral dependence of the filling in due to both atmospheric, $k_a(\lambda)$, and oceanic, $k_w(\lambda)$, Raman scattering is shown in Figure 3. For shorter wavelengths, the ocean filling-in is negative representing a net depletion of energy $k_{w2} > k_{w1}$. The opposite is true at longer wavelengths. The spectral signature is similar for $k_a(\lambda)$ and $k_w(\lambda)$. However, the magnitude of $k_w$ decreases with $\lambda$ owing to decreasing amounts of radiance reaching the surface at excitation wavelengths in the ozone Huggins bands.

[16] The oceanic filling-in substantially depends on absorption by particulate matter and DOM. Figure 4 shows that $k_w$ diminishes rapidly with increasing chlorophyll. This illustrates that there is potential to estimate chlorophyll concentration for Case 1 waters where particulate matter and DOM are highly correlated. Figure 5 shows that $k_w$ decreases with increasing SZA. This dependence is different from that of atmospheric RRS that increases with increasing SZA [*Joiner et al.*, 1995]. The decreasing the oceanic filling-in is explained by reduction of the atmosphere transmittance at excitation wavelengths with increasing SZA. Figure 5 shows that $k_w$ significantly depends on the specification of pure water absorbance.

## 4. Comparison with GOME Observations

[17] Figure 6 shows model results using climatological chlorophyll concentrations from annually averaged Sea-

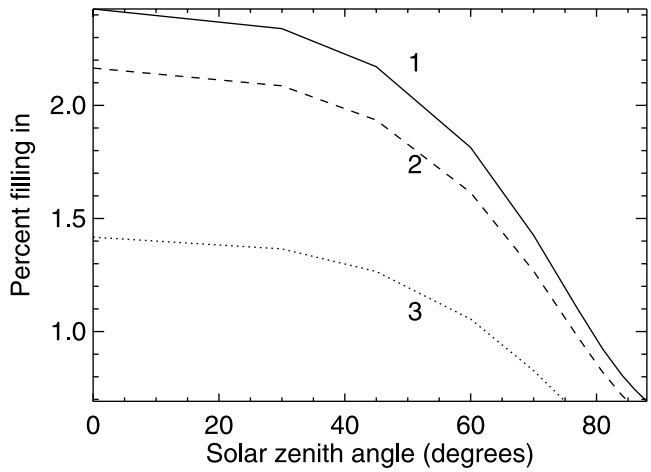


**Figure 5.** $k_w(\theta_o)$ for different estimates of pure water absorbance. 1 – Q&I and P&F interpolation; 2 – extrapolated P&F; 3 – S&B (notations are as in Figure 2).

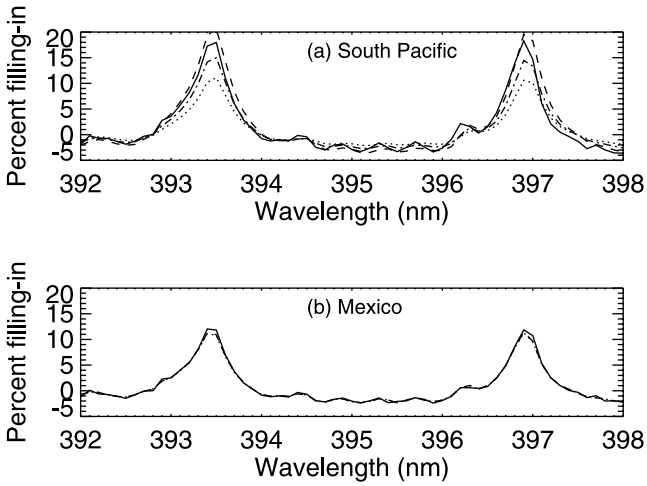


**Figure 6.** GOME spectra from orbit 174 on March 24, 1998 and model calculations. (a) 28°S, 121°W; Solid line – GOME observation; Dashed line – ocean Raman correction with no chlorophyll; Dash dot line – ocean Raman correction with retrieved chlorophyll concentration of 0.084 mg/m$^{-3}$; Dotted line – no ocean Raman correction. (b) 21°N, 108°W; Solid line – GOME observation; Dashed line – ocean Raman correction with climatological chlorophyll concentration of 12.3 mg/m$^{-3}$; Dash dot line – no ocean Raman correction.

WiFS data compared with spectra from the GOME instrument for clear and turbid waters. The low LER reflectivities (12.6% and 6.8%, respectively) indicate relatively cloud-free pixels. In turbid waters off the coast of Mexico, model calculations with and without the ocean Raman contribution differ little. However, in the clear waters of the southern Pacific, observations show a significant difference from model calculations with only atmospheric RRS. Model calculations with zero (climatological) chlorophyll content slightly overestimate (underestimate) the filling-in. The difference between model and observations may be due to a combination of errors in water IOPs and/or the fact that the true chlorophyll content may differ from the climatological value used here. These calculations were performed using the interpolated water absorbance. As Figure 5 indicates, the data are more inconsistent with the measurements of *Smith and Baker* [1981].

## 5. Conclusions and Future Work

[18] Ocean Raman scattering significantly contributes to the total filling-in of solar Fraunhofer lines over clear ocean waters. Our developed model agrees well with observations from GOME and favors pure water absorption interpolated between datasets by *Quickenden and Irvin* [1980] and *Pope and Fry* [1997]. We plan to use the model to estimate of chlorophyll concentration and DOM content from satellite buv observations. This approach is fundamentally different from conventional ocean color algorithms and could be complementary as it has high sensitivity at low chlorophyll concentrations. An advantage of this technique is that because it uses high-frequency spectral structure, it is less affected by errors that have smooth wavelength dependences, such as absolute calibration error.

## References

de Beek, R., M. Vountas, V. V. Rozanov, A. Richter, and J. P. Burrows, The Ring Effect in the cloudy atmosphere, *Geophys. Res. Lett.*, *28*, 721–724, 2001.

Bricaud, A., M. Babin, A. Morel, and H. Claustre, Variability in the chlorophyll-specific absorption coefficients of natural phytoplankton: Analysis and parameterization, *J. Geophys. Res.*, *100*, 13,321–13,332, 1995.

Chance, K. V., and R. D. Spurr, Ring effect studies: Rayleigh scattering, including molecular parameters for rotational Raman scattering, and the Fraunhofer spectrum, *Appl. Opt.*, *36*, 5224–5230, 1997.

Gordon, H. R., Contribution of Raman scattering to water-leaving radiance: A reexamination, *Appl. Opt.*, *38*, 3166–3174, 1999.

Grainger, J. F., and J. Ring, Anomalous Fraunhofer line profiles, *Nature*, *193*, 762, 1962.

Haltrin, V. I., and G. W. Kattawar, Self-consistent solution to the equation of radiative transfer with elastic and inelastic scattering in ocean optics: 1, Model, *Appl. Opt.*, *32*, 5356–5367, 1993.

Joiner, J., and P. K. Bhartia, The determination of cloud pressure from rotational Raman scattering in satellite backscatter ultraviolet measurements, *J. Geophys. Res.*, *100*, 23,019–23,026, 1995.

Joiner, J., P. K. Bhartia, R. P. Cebula, E. Hilsenrath, R. D. McPeters, and H. Park, Rotational Raman scattering (Ring effect) in satellite backscatter ultraviolet measurements, *Appl. Opt.*, *34*, 4513–4525, 1995.

Marshall, B. R., and R. C. Smith, Raman scattering and in-water ocean optical properties, *Appl. Opt.*, *29*, 71–84, 1990.

Morel, A., Optical modeling of the upper ocean in relation to its biogeneous matter content (Case I waters), *J. Geophys. Res.*, *93*, 10,749–10,768, 1988.

Pope, R. M., and E. S. Fry, "Absorption spectrum (380–700 nm) of pure water. II. Integrating cavity measurements,", *Appl. Opt.*, *36*, 8710–8723, 1997.

Quickenden, T. I., and J. A. Irvin, The ultraviolet absorption spectrum of liquid water, *J. Chem. Phys.*, *72*, 4416–4428, 1980.

Sathyendranath, S., and T. Platt, Ocean-color model incorporating transspectral processes, *Appl. Opt.*, *37*, 2216–2227, 1998.

Smith, R. C., and K. C. Baker, Optical properties of the clearest natural waters, *Appl. Opt.*, *20*, 177–186, 1981.

Vasilkov, A. P., N. Krotkov, J. R. Herman, C. McClain, K. Arrigo, and W. Robinson, Global mapping of underwater UV irradiance and DNA-weighted exposures using TOMS and SeaWiFS data products, *J. Geophys. Res.*, *106*(C11), 27,205–27,219, 2001.

Vountas, M., V. V. Rozanov, and J. P. Burrows, Ring effect: Impact of rotational Raman scattering on radiative transfer in Earth's atmosphere, *J. Quant. Spect. Rad. Trans.*, *60*, 943–961, 1998.

A. P. Vasilkov, Science Systems and Applications Inc., Lanham, MD 20706, USA. (alexander_vassilkov@sesda.com)

J. Joiner, J. Gleason, and P. K. Bhartia, Laboratory for Atmospheres, Goddard Space Flight Center, Greenbelt, MD 20771, USA.